A Redox Non-Innocent Ligand Controls the Life Time of a Reactive Quartet Excited State - An MCSCF Study of $[Ni(H)(OH)]^+$

Yavuz Dede,[†] Xinhao Zhang,[‡] Maria Schlangen,[‡] Helmut Schwarz*,[‡] and Mu-Hyun Baik*,[†]

[†]*Department of Chemistry and School of Informatics, Indiana University, Bloomington, Indiana 47405, USA*

[‡]*Institut für Chemie, Technische Universität Berlin, Straße des 17. Juni 135, DE-10623 Berlin, Germany*

email: Helmut.Schwarz@mail.chem.tu-berlin.de, mbaik@indiana.edu

Supporting Information

Table S1. Geometrical parameters (Å and °) of D_0 and Q_1 optimized at B3LYP/LACVP**, CCSD/6-311+G(d,p) and CAS(11,11)/6-311+G(d,p) levels of theory

Geometrical Representation	Internal Coordinate	B3LYP		CCSD		CAS(11,11)		CAS(15,13)	
		D_0	Q_1	D_0	Q_1	D_0	Q_1	D_0	Q_1
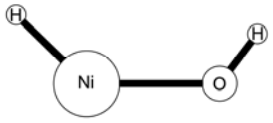	r(H–Ni)	1.428	1.489	1.438	1.489	1.509	1.573	1.464	1.554
	r(Ni–O)	1.690	1.945	1.680	2.015	1.762	2.123	1.704	2.096
	r(O–H)	0.977	0.988	0.969	0.98	0.975	0.985	0.976	0.985
	φ (HNiO)	85.2	119.0	85.3	122.2	86.6	143.6	81.7	135.7
	φ (NiOH)	123.4	125.2	124.9	126.5	120.7	129.1	124.3	127.1
	θ(HNiOH)	-3.2	-0.3	-0.2	-0.1	34.9	-0.1	0.0	-0.3

Table S2. Electronic, ZPVE corrected, and entropy corrected relative energies (kcal mol^{-1}) of the quartet and doublet states (Q_1 - D_0) of $[H–Ni–OH]^+$ at various levels of theory

Theoretical Level	ΔE(SCF)	ΔH_0	ΔG_0
B3LYP/LACVP**	19.60	17.58	16.13
CCSD(T)/6-311++G(3d,2p)	24.47	22.45	20.88
CAS(11,11)/6-311+G(d,p)	16.87	14.86	13.26
MRMP(11,11)/6-311+G(d,p)	25.93	23.92	22.32
CAS(15,13)/6-311+G(d,p)	20.70	18.69	17.09
MRMP(15,13)/6-311+G(d,p)	34.70	32.69	31.08

CCSD(T) calculations used CCSD/6-311+G(d,p) optimized geometries. MRMP calculations used CAS optimized geometries.

Table S3. Geometrical parameters (Å and °) of the two CPs, D_0, Q_1, and D_1 optimized at CAS(11,11)/6-311+G(d,p) level of theory

Geometrical Representation	Internal Coordinate	CP	CP[1 a]	D_0	Q_1	D_1
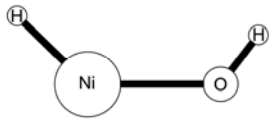	r(H–Ni)	1.576	1.556	1.509	1.573	1.538
	r(Ni–O)	2.118	1.947	1.762	2.123	1.771
	r(O–H)	0.985	0.980	0.975	0.985	0.974
	φ (HNiO)	135.3	115.5	86.6	143.6	87.5
	φ (NiOH)	129.5	125.0	120.7	129.1	120.9
	θ(HNiOH)	23.2	0.0	34.9	-0.1	0.0

[a] *Crossing Point of Q_1 and D_1 surfaces.*

Table S4. Relative electronic energies (kcal mol^{-1}) of the Q_1 ,D_1 and D_0 states of $[H–Ni–OH]^+$ at CAS(11,11), CAS(15,13)//CAS(11,11) and CAS(15,13) levels of theory

	ΔE(SCF) kcal mol^{-1})		
	(11,11)	(15,13)//(11,11)	(15,13)
Q_1	16.87	18.08	20.07
D_1	8.65	7.83	[a]
D_0	0.00	0.00	0.00

[a] *Not computed*

Table S5. Relative electronic energy (kcal mol^{-1}) comparison of the Q_1 and D_0 states of $[H–Ni–OH]^+$ at CAS(15,13) and CCSD(T) levels of theory

	ΔE(SCF) Q – D (kcal mol^{-1})		
E(SCF)	CCSD(T)	CAS(15,13)	MRMP(15,13)
CCSD Geometry	24.47	21.77	31.72
CAS(15,13) Geometry	26.34	20.70	34.70

6-311+G(d,p) basis is used for MRMP and CAS; 6-311++G(3d,2p) for CCSD(T) single point energy calculations. CCSD geometry optimizations wee done with 6-311+G(d,p) basis set.

Table S6. Relative electronic energies of D_0, D_1 and Q_1 states at the, Q_1 - D_0 CP geometry in kcal mol^{-1} at CAS(11,11) and MRMP(11,11) levels of theory

	ΔE(SCF) (kcal mol^{-1})	
State	CAS	MRMP
Q_1	17.13	25.98
D_1	21.44	31.55
D_0	17.36	25.91

Energies are relative to D_0 equilibrium.

Table S7. Relative electronic energies and geometrical parameters (Å and °) of D_4 and Q_5 states optimized at CAS(11,11)/6-311+G(d,p) level of theory

		D_4	Q_5
	ΔE(SCF) (kcal mol^{-1})	60.0	56.2
Geometrical Representation	Geometrical Parameters		
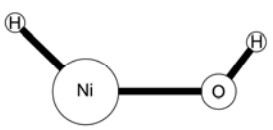	r(H–Ni)	1.494	1.581
	r(Ni–O)	2.018	2.095
	r(O–H)	0.983	0.984
	φ (HNiO)	106.2	162.2
	φ (NiOH)	133.3	138.6
	θ(HNiOH)	0.0	0.0

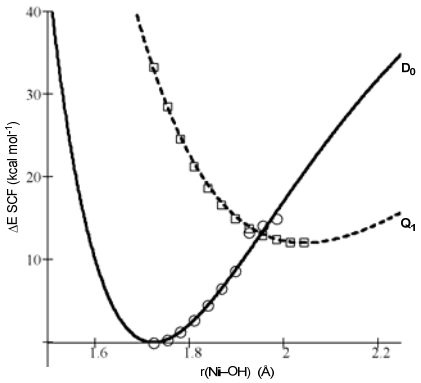

Figure S1. Potential energy surfaces of the lowest doublet and quartet states at CAS(13,13)/cc-pVTZ level. Only one coordinate r(Ni–O) is shown on the x axes.

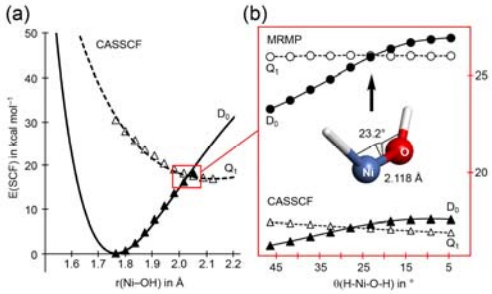

Figure S2. Potential energy surfaces of the lowest doublet and quartet states at CAS(11,11)/6-311+G(d,p) and MRMP(11,11)/6-311+G(d,p)level. Only the most affected coordinates r(Ni–O) and θ(HNiOH) are shown on the x axes in (a) and (b) respectively.

Table S8. Spin orbit coupling constants calculated at CAS(11,11) level of theory at the relevant CPs

States	$D_0 - Q_1$	$D_1 - Q_1$
Geometry	CP ($D_0 - Q_1$)	CP^1($D_1 - Q_1$)
SOCC (cm^{-1})	16.8	416. 7

Table S9. Isosurface plots with NOONs for orbitals 12 to 20 of D_0 and Q_1 at the CP

NO	D_0 CP	NOON	Q_1 CP	NOON
20	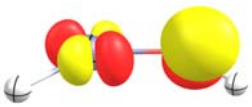	0.85	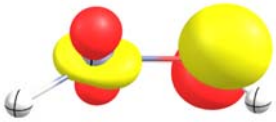	1.00
19	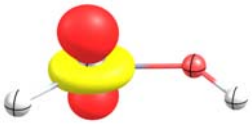	1.00	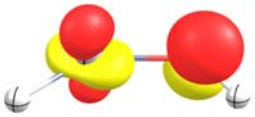	1.00
18		1.15	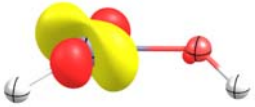	1.00
17	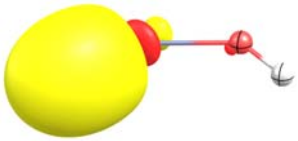	1.98	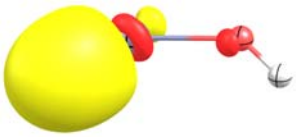	1.95
16	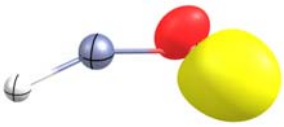	1.98	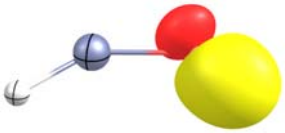	1.98
15	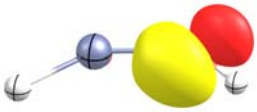	1.98	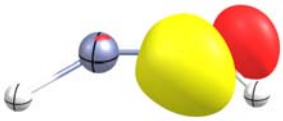	1.98
14	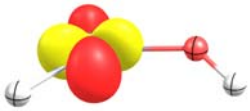	1.99	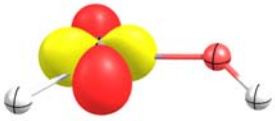	1.99
13	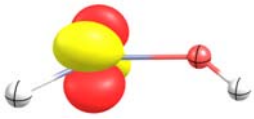	2.00	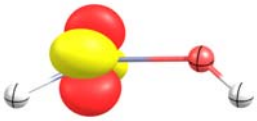	2.00
12	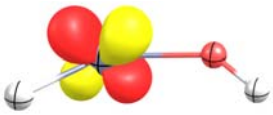	2.00	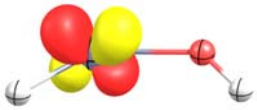	2.00

CAS (11,11) geometries are used. NOs 12 and 13 make the two highest lying orbitals of the MCSCF core. NOs 14 through 16 are essentially doubly occupied and NOs 21 to 24 are unoccupied for both states.

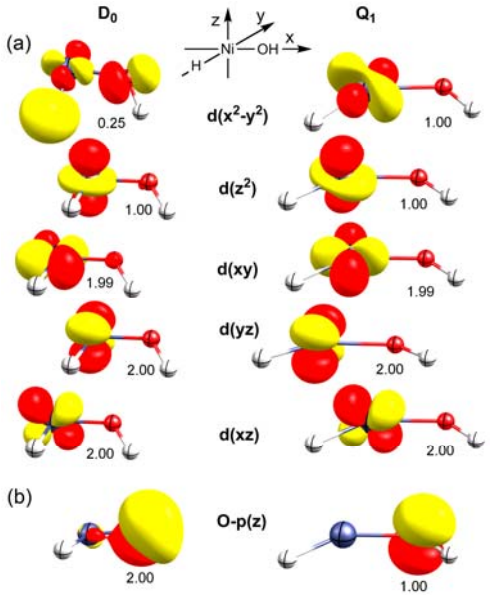

Figure S3. Isosurface plots (isodensity value = 0.075 a.u) and occupation numbers of the most important natural orbitals, for the D_0 and Q_1 states of $[Ni(H)(OH)]^+$ at CAS(11,11)/6-311+G(d,p) level.

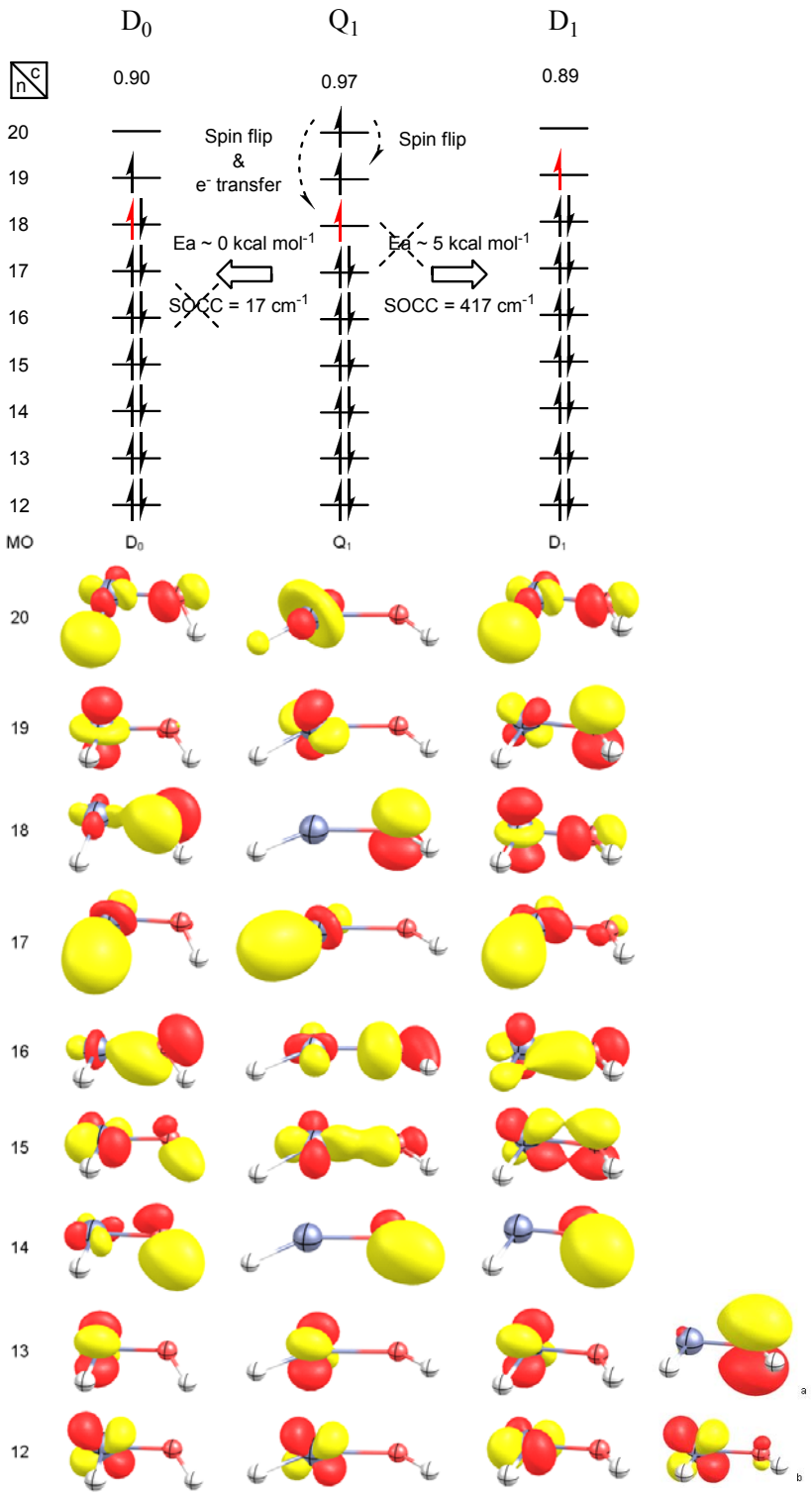

Figure S4. top: Dominant CASSCF CSFs with coefficients (c) on top and canonical MO indexes (n) on left. bottom: CASSCF canonical MO isosurface plots.

MOs 21 to 24 are empty for all three states. [a] *Obtained by addition of isosurfaces for MO 15 and 19 for* D_1. [b] *Obtained by subtraction of isosurfaces for MO 15 and 19 for* D_1.

The large difference in the SOCCs of Q_1 with D_0 and D_1 is not clear at first glance as D_1 resembles D_0 in the sense that it has a single unpaired electron. A more detailed analysis of the MOs show that MO 19 hosting the odd electron in D_1 is not the Ni dominated MO 19 in D_0 but rather an orbital having more oxygen-*p*(z) character (Figure S1). Thus the formal assignment D_x in Figure 3 of the main text is mostly representing D_1 and the large SOCC is the result of Ni nucleus acting on an electron residing in Ni dominated orbitals by pairing two α electrons in the Q_1 state or unpairing two electrons of D_1. This local spin inversion is expected on the order of a few hundred cm^{-1}, in agreement with our computations, as a TM is involved. This assignment is made by using the CSFs with ~ 80 % weights in the CI expansion. For all important expansions see Figure S2. One may also think that using larger active spaces by which one can locate additional excited states between D_0 and D_1 may be possible. Such a scenario should yield the important D_1 to be a higher excited state and would still yield low SOCCs between Q_1 and D_n unless significant electronic structure match with Q_1 develops in D_n.

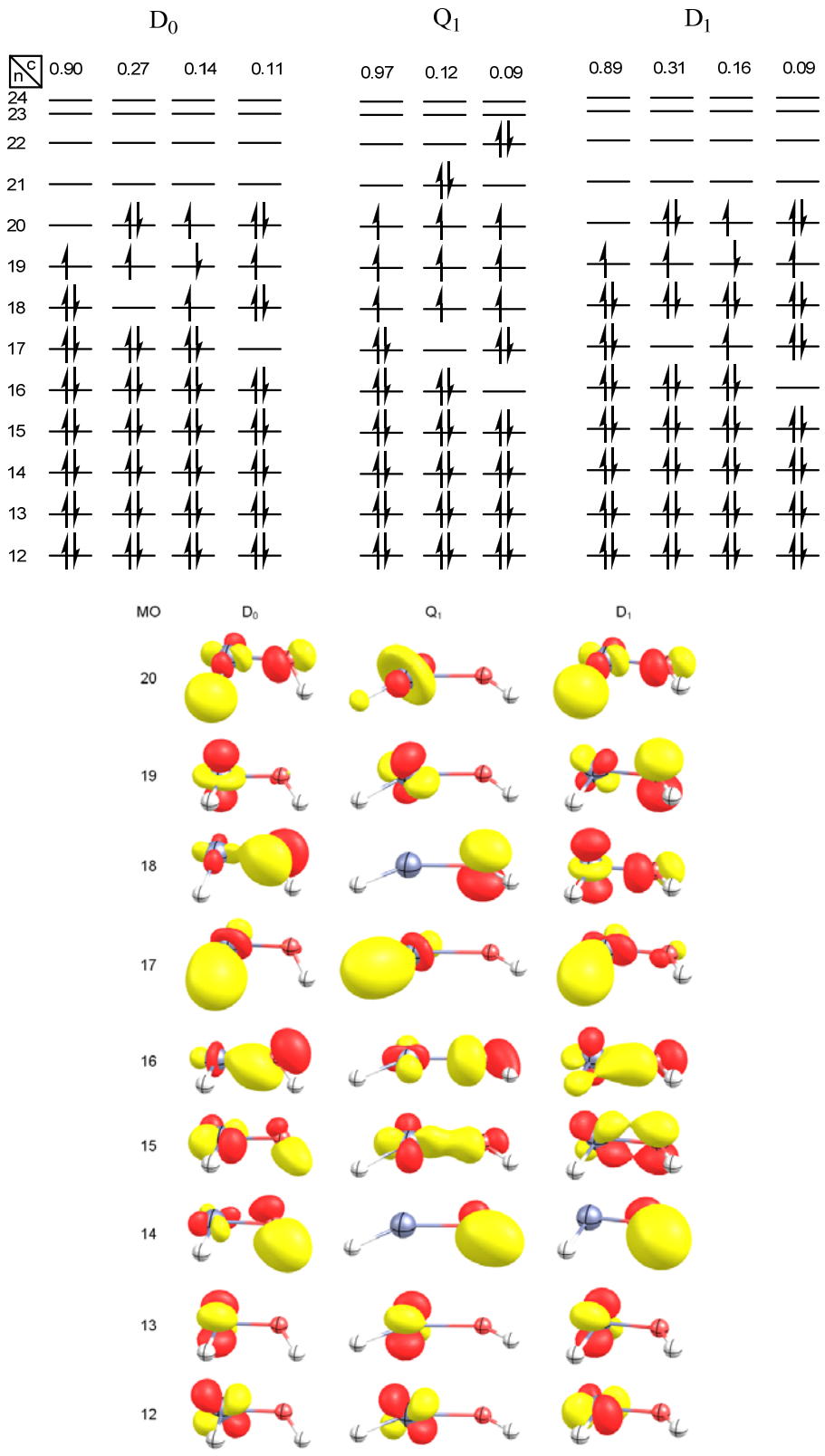

Figure S5. top: CASSCF CSFs with coefficients (c) on top and canonical MO indexes (n) on left. CSFs with coefficients larger than 0.08 (0.06 %) are shown. bottom: CASSCF canonical MO isosurface plots.

Table S10. Isosurface plots with natural orbital occupation numbers (NOON) for orbitals 12 to 20 of the quartet and doublet [H–Ni–OH]$^+$ at MRMP(15,13) level of theory

NO	D_0	NOON	Q_1	NOON
20	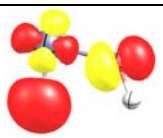	0.19		1.00
19	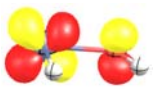	1.04	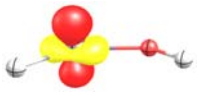	1.01
18		1.86	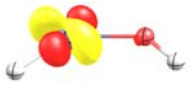	1.01
17		1.95		1.98
16	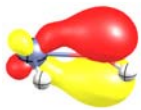	1.96	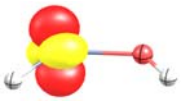	1.98
15		1.98	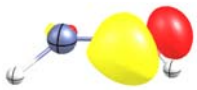	1.98
14	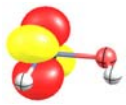	1.98		1.99
13		1.98	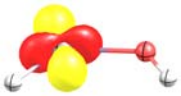	1.99
12		1.98		1.99

Geometries are at CAS(15,13) level. Contour value is at 0.075 a.u. NOs 21 to 24 are unoccupied for both states.

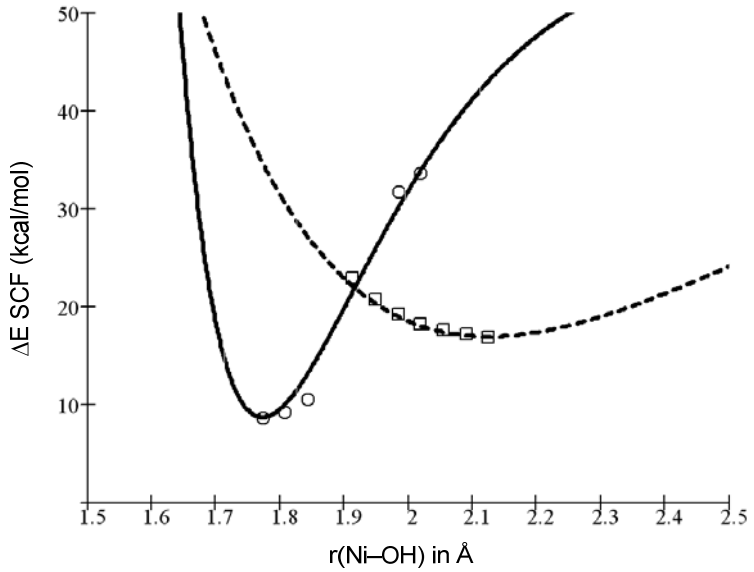

Figure S6. PES scan along the vector connecting Q_1 and D_1 at CAS(11,11)/6-311+G(d,p) level.

Energies are relative to D_0. CP^1 lies 5.5 kcal mol^{-1} higher than Q_1.

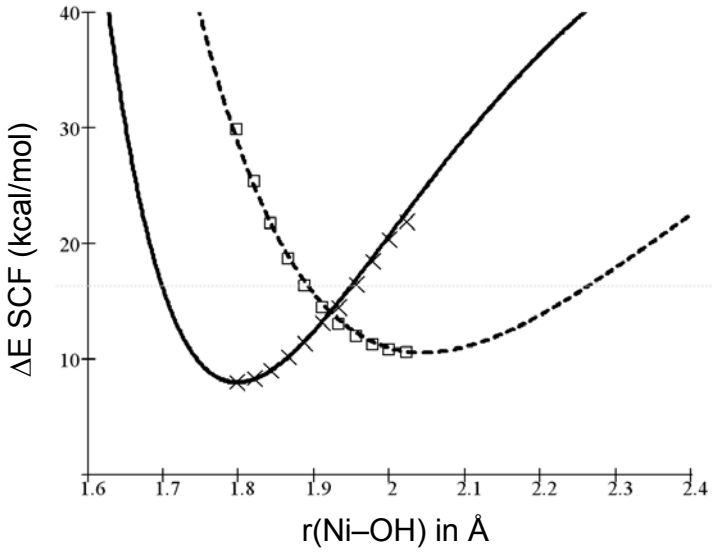

Figure S7. PES scan along the vector connecting Q_1 and D_1 at CAS(13,13)/cc-pVTZ level.

Energies are relative to D_0. CP^1 lies 3.9 kcal mol^{-1} higher than Q_1.

Table S11. Selected CAS(11,11) CI coefficients (c) and NOONs of NOs 14 to 21 for D_4, and Q_5

				14	15	16	17	18	19	20	21
	c			NOON							
D_4	0.70	0.27	0.25	1.98	1.94	1.66	1.60	1.53	1.37	0.82	0.05
Q_5	0.96			1.98	1.95	1.60	1.40	1.39	1.39	1.20	0.05

CI coefficients larger than 0.2 are given. NOs 22 to 24 are empty for all three states.

Probability and rate calculations

The nonadiabatic transition probability with the Airy function to approximate the overlap of vibrational wavefunctions and include tunneling effects is given as

$$p(\varepsilon_t) = \Pi^2 \beta^{4/3} A_i^2\left(-\varepsilon\beta^{2/3}\right)$$

where the dimensionless variables β, ε, ε_0 are defined as:

$$\beta = \frac{4H_{12}^{3/2}}{\hbar}\left(\frac{\mu}{F\Delta F}\right)^{1/2} \qquad \varepsilon = \left(\varepsilon_t - E_c\right)\varepsilon_0 \qquad \varepsilon_0 = \frac{\Delta F}{2FH_{12}}$$

and the slopes F_1 and F_2 of the two PESs at the crossing define $\Delta F = \left|F_1 - F_2\right|$ and $F = \left|F_1 F_2\right|^{1/2}$. Here H_{12} is the SOCC, E_c is the energy of the crossing and ε_t the initial energy of the molecule. The probabilities of ISC (Table S10) were used as a pre-exponential factor for thestandard rate equation, where k_β is the Boltzman constant and T the temperature. The parameters and constants used in the equations are given in Table S13.

$$k(t) = p(\varepsilon_t) k_\beta T h^{-1} \exp\left(\frac{-E_a}{RT}\right)$$

Table S12. Calculated probabilities, $p(\varepsilon_t)$ for ISCs.

States	$p(\varepsilon_t)$	E_a (kcal mol^{-1})	$t_{1/2}$ (sec)
$Q_1 \rightarrow D_0$	2.8×10^{-6}	1.1	2.6×10^{-7}
$Q_1 \rightarrow D_0$	7.7×10^{-13}	2.6	1.2×10^{1}
$Q_1 \rightarrow D_1$	1.8×10^{-17}	3.9	5.3×10^{6}

The gradients of the two surfaces in Q_1–D_0 transformation (in atomic units) are 0.0136 and -0.0023 at the crossing. The reduced masses for the two states, since computed with the spin pure wavefunctions and with the harmonic approximation are highly approximate. With

this approximations in mind the expected motion to hop from the Q_1 to D_0 would show a significant amount of Ni–O bond shortening. Although a vibrational mode is delocalized over the entire molecule two similar character vibrations with similar frequencies and reduced masses can be extracted from the analysis and the arithmetic mean of these two reduced masses is used for the probability calculation, which is 3.49 amu. It is important to note that a very localized Ni–O contraction would have higher reduced masses, close to 16 amu, i.e. the mass of oxygen and this would yield an even lower ISC probability and predict a lifetime of 7.1×10^{-5} seconds for Q_1 using an E_a of 1.1 kcal mol^{-1}. Note that two decay routes of Q_1 are essentially blocked for barriers above 2 kcal mol^{-1}.

Table S13. Details of the parameters and constants used in the RRKM calculations.

Variable or Constant	Units	Value
F_1	AU[a]	0.0136
F_2	AU[a]	-0.0023
μ	AU[a]	3.49
R	J K^{-1} mol^{-1}	8.314
k_β	kg m^2 s^{-2} K^{-1}	1.38×10^{-23}
h	Js	6.626×10^{-34}

[a] Atomic units

Table S14. Calculated probabilities, $p(\varepsilon_t)$ for a range of activation energies for Q_1–D_0 ISC.

$p(\varepsilon_t)$	E_a (kcal mol^{-1})
0.14	1.1×10^{-3}
0.28	5.6×10^{-4}
0.42	2.6×10^{-4}
0.57	1.1×10^{-4}
0.71	4.5×10^{-5}
0.86	1.7×10^{-5}
1.00	5.7×10^{-6}
1.14	1.8×10^{-6}
1.29	5.5×10^{-7}
1.43	1.6×10^{-7}
1.58	4.2×10^{-8}
1.72	1.1×10^{-8}
1.86	2.5×10^{-9}
2.01	5.7×10^{-10}
2.15	1.2×10^{-10}
2.30	2.5×10^{-11}
2.44	5.0×10^{-12}
2.58	9.3×10^{-13}
2.73	1.7×10^{-13}
2.87	2.8×10^{-14}
3.02	4.7×10^{-15}

Cartesian Coordinates and Absolute Energies of the Species Discussed

D_0
B3LYP/cc-pVTZ -1584.504536

O	0.066358000	0.004542000	0.245864000
Ni	-0.207165000	-0.005839000	1.900851000
H	1.221524000	0.005900000	2.055758000
H	0.952629000	0.015619000	-0.158686000

Q_1
B3LYP/cc-pVTZ -1584.4733584

O	-0.001045000	0.005721000	0.025944000
Ni	0.174388000	-0.002987000	1.737039000
H	1.169529000	0.000679000	2.943971000
H	0.690474000	0.016810000	-0.663169000

D_0
CCSD/6-311+G(d,p)

Ni	-0.009680000	-0.000891000	-0.014002000
H	0.020819000	0.000598000	1.423498000
O	1.666661000	0.001319000	0.089147000
H	2.171066000	0.005928000	0.916601000

Q_1
CCSD/6-311+G(d,p)

O	0.008759000	0.005750000	-0.055629000
Ni	-0.014460000	-0.004502000	1.959702000
H	1.235948000	0.001968000	2.768362000
H	0.803099000	0.017006000	-0.628649000

Q_1
CAS(15,13)/6-311+G(d,p) -1582.5868232311

O	-0.014370301	0.005260564	-0.143301411
Ni	0.083971849	-0.002936562	1.950472559
H	1.220664426	0.000175090	3.009950636
H	0.743080026	0.017722908	-0.773335783

D_0
CAS(15,13)/6-311+G(d,p)

H	0.066552058	-0.000405576	1.423579064
Ni	-0.034362787	-0.003717386	-0.036656082
O	1.664543077	0.003384539	0.091688127
H	2.152133650	0.007692423	0.936632890

D_0

CCSD(T)//CCSD/cc-pVTZ -1583.2345605

H	0.088618000	0.001046000	1.400256000
Ni	-0.022071000	-0.001402000	-0.022498000
O	1.647057000	0.002012000	0.101249000
H	2.135262000	0.005299000	0.936237000

Q_1
CCSD(T)//CCSD/cc-pVTZ -1583.1942133

O	0.000436000	0.006138000	-0.048673000
Ni	-0.015123000	-0.004805000	1.943404000
H	1.237437000	0.002307000	2.747098000
H	0.810596000	0.016582000	-0.598043000

D_0
B3LYP/aug-cc-pVTZ -1584.5068699

Ni	-0.003681000	-0.001454000	-0.008948000
H	0.003885000	0.000978000	1.429283000
O	1.672891000	0.002209000	0.080042000
H	2.175770000	0.005222000	0.914867000

Q_1
B3LYP/aug-cc-pVTZ -1584.4756796

Ni	0.175271000	-0.001797000	1.735202000
H	1.163655000	0.000548000	2.948639000
O	0.001890000	0.006021000	0.024925000
H	0.692530000	0.015450000	-0.664979000

Q_1
CAS(13,13)/cc-pVTZ

H	1.219868166	0.002358909	2.884179890
Ni	0.035694582	-0.004175697	1.959428434
O	0.028243187	0.006595818	-0.083182504
H	0.749540063	0.015442971	-0.716639822

D_0
CAS(13,13)/cc-pVTZ -1582.778869

H	1.405797871	0.008100798	2.144769631
Ni	-0.006221683	-0.004178085	1.833988201
O	0.465129384	0.009917933	0.176414904
H	1.367920179	0.018057365	-0.127629971

D_0
OPBE/6-311+G(d,p) -1584.7010384

H	0.018946000	0.001006000	1.425154000
Ni	-0.007149000	-0.001454000	-0.007372000
O	1.676070000	0.002193000	0.074522000
H	2.160998000	0.005210000	0.922939000

Q_1
OPBE/6-311+G(d,p) -1584.6658745

H	1.157004000	0.000359000	2.962747000
Ni	0.193957000	-0.001695000	1.737951000
O	-0.002831000	0.005657000	0.019255000
H	0.685216000	0.015901000	-0.676167000

D_0
OPBE/cc-pVTZ -1584.827156

H	0.045465694	-0.002205060	1.420711459
Ni	-0.004085987	-0.000062268	-0.007722793
O	1.672037489	0.004164340	0.071357706
H	2.135448686	0.005058059	0.930897911

Q_1
OPBE/cc-pVTZ -1584.793127

H	1.164811453	0.000718079	2.918157663
Ni	0.165814781	-0.001993010	1.729264799
O	-0.018721608	0.005611860	0.017926103
H	0.721441660	0.015885232	-0.621562313

MEX
OPBE/cc-pVTZ -1584.792277

H	1.232316968	-1.311313291	-0.069176282
Ni	0.251096333	-0.128260055	-0.056863194
O	-1.460148422	0.066832795	0.056875794
H	-2.086589266	-0.681651884	0.128640918

Q_1
B3LYP/cc-pVQZ -1584.484891

H	1.161961000	0.000433000	2.950608000
Ni	0.176720000	-0.001972000	1.734555000
O	0.004023000	0.005612000	0.025428000
H	0.690642000	0.016150000	-0.666805000

D_0
B3LYP/cc-pVQZ

H	0.003828000	0.000982000	1.429252000
Ni	-0.002972000	-0.001460000	-0.008827000
O	1.672625000	0.002221000	0.080688000
H	2.175385000	0.005212000	0.914131000

Q_1

B3LYP/6-311+G(d,p) -1584.352535

H	1.146543000	0.000072000	2.998726000
Ni	0.207791000	-0.001582000	1.737894000
O	0.022549000	0.005876000	0.025066000
H	0.656462000	0.015855000	-0.717900000

D_1
CAS(13,13)/cc-pVTZ

H	0.054898078	0.007945092	1.417852375
Ni	-0.080912799	-0.009241143	-0.033578998
O	1.710155115	-0.002097024	0.097313157
H	2.164725603	0.010347075	0.933657466

Complete Reference 4 and 26

(4) Arakawa, H.; Aresta, M.; Armor, J. N.; Barteau, M. A.; Beckman, E. J.; Bell, A. T.; Bercaw, J. E.; Creutz, C.; Dinjus, E.; Dixon, D. A.; Domen, K.; DuBois, D. L.; Eckert, J.; Fujita, E.; Gibson, D. H.; Goddard, W. A.; Goodman, D. W.; Keller, J.; Kubas, G. J.; Kung, H. H.; Lyons, J. E.; Manzer, L. E.; Marks, T. J.; Morokuma, K.; Nicholas, K. M.; Periana, R.; Que, L.; Rostrup-Nielson, J.; Sachtler, W. M. H.; Schmidt, L. D.; Sen, A.; Somorjai, G. A.; Stair, P. C.; Stults, B. R.; Tumas, W., *Chem. Rev.* **2001,** *101*, 953-996.

(48) Frisch, M. J.; Trucks, G. W.; Schlegel, H. B.; Scuseria, G. E.; Robb, M. A.; Cheeseman, J. R.; Montgomery, J., J. A.; Vreven, T.; Kudin, K. N.; Burant, J. C.; Millam, J. M.; Iyengar, S. S.; Tomasi, J.; Barone, V.; Mennucci, B.; Cossi, M.; Scalmani, G.; Rega, N.; Petersson, G. A.; Nakatsuji, H.; Hada, M.; Ehara, M.; Toyota, K.; Fukuda, R.; Hasegawa, J.; Ishida, M.; Nakajima, T.; Honda, Y.; Kitao, O.; Nakai, H.; Klene, M.; Li, X.; Knox, J. E.; Hratchian, H. P.; Cross, J. B.; Bakken, V.; Adamo, C.; Jaramillo, J.; Gomperts, R.; Stratmann, R. E.; Yazyev, O.; Austin, A. J.; Cammi, R.; Pomelli, C.; Ochterski, J. W.; Ayala, P. Y.; Morokuma, K.; Voth, G. A.; Salvador, P.; Dannenberg, J. J.; Zakrzewski, V. G.; Dapprich, S.; Daniels, A. D.; Strain, M. C.; Farkas, O.; Malick, D. K.; Rabuck, A. D.; Raghavachari, K.; Foresman, J. B.; Ortiz, J. V.; Cui, Q.; Baboul, A. G.; Clifford, S.; Cioslowski, J.; Stefanov, B. B.; Liu, G.; Liashenko, A.; Piskorz, P.; Komaromi, I.; Martin, R. L.; Fox, D. J.; Keith, T.; Al-Laham, M. A.; Peng, C. Y.; Nanayakkara, A.; Challacombe, M.; Gill, P. M. W.; Johnson, B.; Chen, W.; Wong, M. W.; Gonzalez, C.; Pople, J. A., ed.; Gaussian03, Revision C.02., Gaussian Inc., Wallingford: 2004; 'Vol.' p.